NMR IMAGING

DAVID MORATAL
Universitat Politècnica de València
Valencia, Spain
MARIJN E. BRUMMER
Emory University School of Medicine
Atlanta, Georgia
LUIS MARTÍ-BONMATÍ
Hospital Universitari Dr. Peset
Valencia, Spain
ANA VALLÉS-LLUCH
Universitat Politècnica de València
Valencia, Spain

1. INTRODUCTION

The nuclear magnetic resonance physical principles can be summarized as four phenomena: *polarization*, which describes the equilibrium tendency of nuclear magnetic moments to align parallel with an external magnetic field; *excitation*, which describes how an aggregate net magnetization of a collection of nuclear spins can be tipped out of equilibrium by the application of a radiofrequency (RF) electromagnetic wave pulse; *precession*, which describes how non-equilibrium magnetization resonates within the magnetic field and, finally, *relaxation*, which explains how the magnetization returns to equilibrium. The following sections will present some details on each of these phenomena.

2. POLARIZATION

The magnetism has its origin in the movement of electrically charged particles. Magnetization refers to the phenomenon caused by a non-random orientation of the magnetic moment of the electrons. This orientation results in a net magnetization. In addition to electrons, most of the atomic nuclei possess a small field or magnetic moment which is used for obtaining MR (magnetic resonance) images (Fig. 1). This nuclear magnetism has its origin in the nuclear spin and its associated angular momentum which is related to the atomic number (number of protons), to the atomic mass (number of protons plus number of neutrons) and to the number of neutrons. A net nuclear magnetic moment is present in atoms with an odd number of nucleons, i.e., either when the number of protons is odd and the number of neutrons is even number, as is the case for ^{1}H (hydrogen-1), ^{15}N (nitrogen-15), ^{19}F (fluorine-19), ^{23}Na (sodium-23), and ^{31}P (phosphorus-31), or when the number of protons is even and the number of neutrons is odd, as for ^{13}C (carbon-13). The hydrogen, with just one proton (^{1}H) is a good isotope for imaging because of its great natural abundance in the living matter and because it has a larger nuclear magnetic moment than any other atom, resulting in an easily detectable signal.

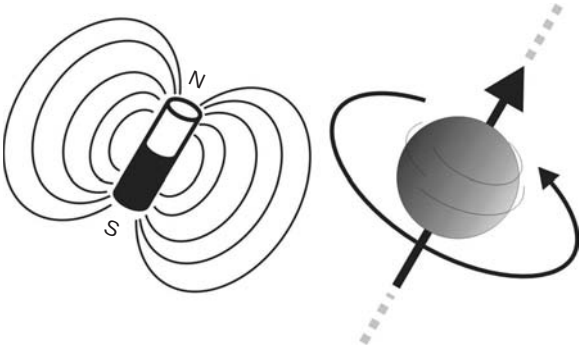

Figure 1. The nuclei of some atoms have a magnetic moment, which can be thought of as a small magnet with a north and south pole. Nuclear magnetism arises from an intrinsic property of the nucleus called spin angular momentum, or spin.

In biological samples, the protons essential to conventional MR imaging are either in water or in lipid molecules.

As described above, atoms with an odd number of protons or neutrons possess an intrinsic characteristic known as spin-angular momentum. The magnetic moment from individual atoms is very weak and cannot be detected with conventional technology. Normally the nuclear "spins" are randomly aligned, so that there is no net magnetization in a material, as shown in Fig. 2a. Magnetism of the necessary strength can be created by aligning the spins of many atoms, causing their magnetism to act in coherently. When the collection of spins is placed in a strong magnetic field, typically indicated by the parameter $\mathbf{B_0}$, the spins align either along or opposite to the magnetic field (Fig. 2b). Overall, ^{1}H spins tend to align with the magnetic field by a very small number (lower energy level, see Fig. 2c), providing a net magnetic moment. This net magnetic moment, or net magnetization, will be the basis of the signal in NMR or MRI. The strength of $\mathbf{B_0}$ used in MR imaging varies between 0.15 and 9.7 Tesla (T), but the most common field strength in clinical MRI is currently 1.5 T. For reference, the earth's magnetic field is approximately 0.5-1 Gauss, and 1 T is equivalent to 10,000 Gauss.

In presence of a static magnetic field, protons populate two distinct energy levels (E_1 and E_2), as depicted in Fig. 2c. The energy difference between these levels (ΔE) increases linearly with magnetic field strength, as does the population difference (p_1 and p_2). A spin's state can jump to the high energy level if it receives an external energy equal or greater than ΔE (energy separation between these two levels). This process is called excitation. After having received that external energy, the spin will tend to return to its equilibrium (lower energy level), emitting the previously absorbed energy. This process is called relaxation. The energy difference can be calculated as $\Delta E = h \cdot \omega$, where $h = 6.62 \times 10^{-34}\,\mathrm{J \cdot s}$. If we increase the field strength we increase the energy difference and hence also the population difference (p_1 *vs.* p_2). Since the size of the NMR signal is directly dependent on the population difference, the NMR signal also increases. This explains in part an increase of the signal-to-noise ratio of NMR signals with field strength.

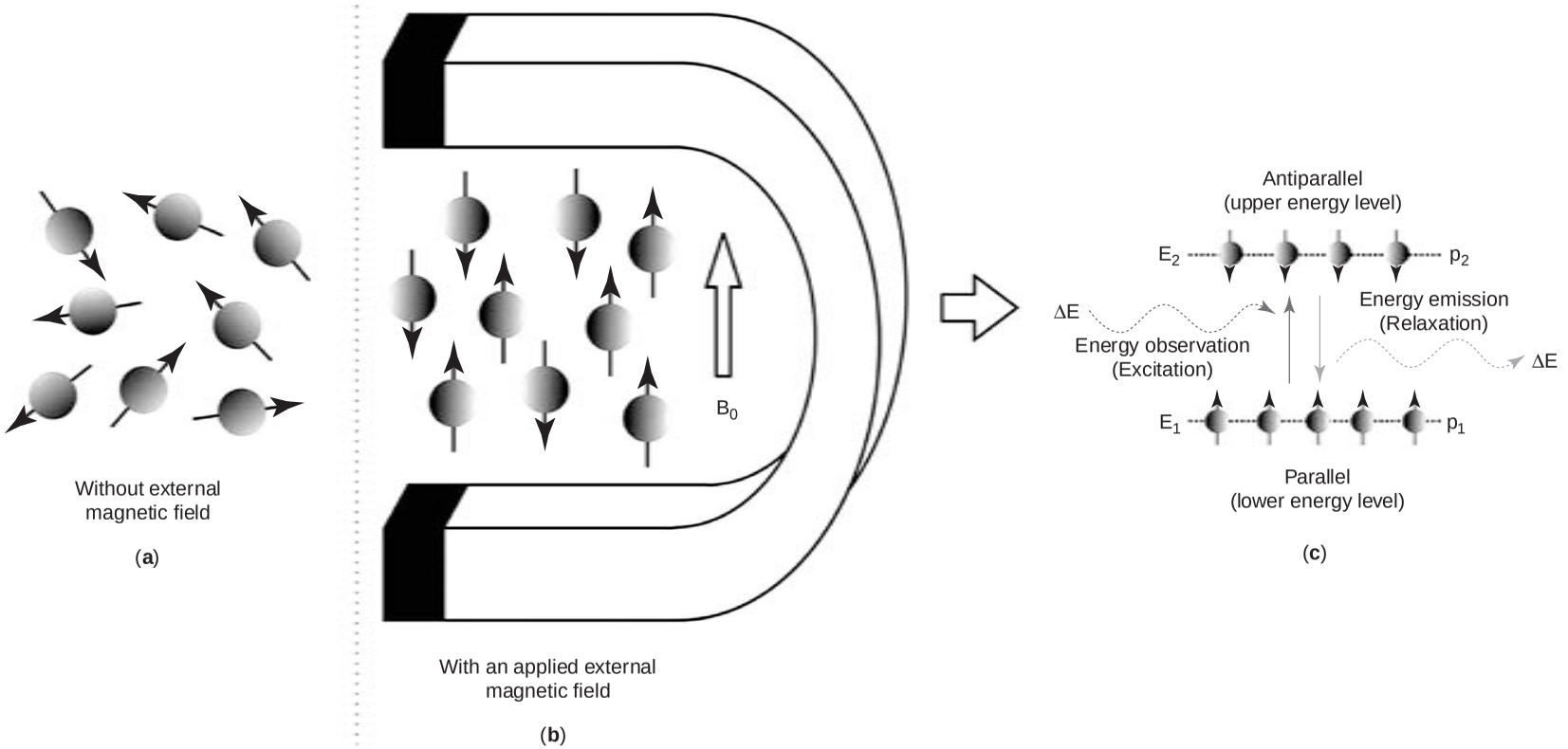

Figure 2. (a) Magnetic moments of a material outside of a magnetic field are aligned randomly (no net magnetic moment exists). (b) With the application of a strong magnetic field, $\mathbf{B_0}$, these moments align either with (parallel) or against (antiparallel) the direction of that magnetic field. Overall, spins tend to align with the magnetic field by a very small number, providing a net magnetic moment (net magnetization), being the basis of the MR signal. (c) Under the application of a strong magnetic field, nuclei populate two distinct energy levels: the lower energy level if the spin aligns with the magnetic field and the upper energy level if the spin aligns against the magnetic field. A spin can jump from the lower energy level to the upper energy level absorbing the energy difference, ΔE (excitation) or from the upper energy level to the lower energy level emitting the energy difference, ΔE (relaxation). This situation of only two allowed states is true only for nuclei whose "magnetic spin quantum number" is equal to 1/2. This includes ^{1}H, ^{13}C, ^{19}F and ^{31}P among others. Other magnetically active nuclei, e.g. ^{2}H and ^{23}Na, are allowed more than two orientations. (This figure is available in full color at http://www.mrw.interscience.wiley.com/ebe.)

In a quantum-mechanical sense, radiofrequency (RF) waves may be considered as packets of energy. If that packet of energy equals ΔE it will cause a spin to jump to the high energy level. After an RF pulse, many spins will transit to the higher energy state, and there will be no longer an equilibrium state. To return to this state, the spins which jumped to the higher energy state have to return to the low level. In doing so, such spins will emit an amount of energy, ΔE, which in aggregate will be detectable as an RF signal in an NMR experiment. The transitions back to the equilibrium do not all occur immediately, but extend over a period of time following the RF pulse.

2.1. The Bloch Equation

In a static magnetic field $\mathbf{B_0}$, traditionally described as oriented along the z-axis of a Cartesian coordinate frame, the dynamics of the magnetization are described by the Bloch equation,

$$\frac{d\mathbf{M}}{dt} = (\mathrm{M} \times \gamma \mathbf{B}_0) + \frac{\mathbf{M}_0 - \mathbf{M}_z}{\mathrm{T}_1} - \frac{\mathbf{M_{xy}}}{\mathrm{T}_2}, \quad (1)$$

where the x-y plane represents the transverse plane perpendicular to the main magnetic field. $\mathbf{M}$ represents the time-varying magnetization vector, $\mathbf{M_0}$ is the equilibrium magnetization vector that results from the magnetic field $\mathbf{B_0}$, $\mathbf{M_{xy}}$ is the component of the magnetization in the transverse plane and $\mathbf{M_z}$ is the component of the magnetization along the direction of the magnetic field. The longitudinal and transverse relaxation times, T_1 and T_2 and the gyromagnetic ratio, γ, are constants that depend on the material being imaged. The relaxation times, T_1 and T_2, are parameters of molecular structures; T_1 is always greater than T_2.

3. PRECESSION

The first term of the Bloch equation describes precession, or resonance: $\frac{d\mathbf{M}}{dt} = \mathrm{M} \times \gamma \mathbf{B}$. In the absence of an external magnetic field, the spins are randomly oriented, but when placed in a strong magnetic field, a small fraction of the spins align with the axis of the applied field, resulting in a net magnetization, $\mathbf{M_z}$, in the longitudinal direction (z-axis). These spins precess about the z axis at a frequency directly proportional to the strength of the magnetic field, as shown in Fig. 3. The Larmor equation

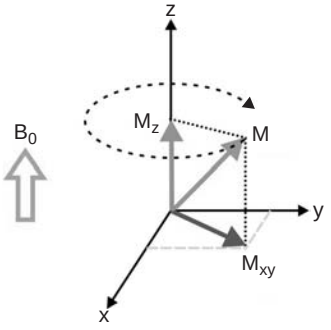

Figure 3. The magnetization vector precesses about the direction of the applied magnetic field at a rate that is proportional to the strength of the applied magnetic field, $\mathbf{B_0}$. $\mathbf{M_{xy}}$: transverse component of the magnetization, $\mathbf{M}$. $\mathbf{M_z}$: longitudinal component of the magnetization, $\mathbf{M}$. (This figure is available in full color at http://www.mrw.interscience.wiley.com/ebe.)

describes the dependence between the magnetic field, $\mathbf{B_0}$, and the angular frequency, $\grave{u}_0$, known as the Larmor frequency:

$$\omega_o = \gamma |\mathbf{B_0}|. \quad (2)$$

The gyromagnetic ratio, γ is a material constant, and has a value of 42.5781 MHz/T for ^{1}H (see Table 1). Hydrogen protons are most commonly imaged due to their abundance in living tissue.

4. EXCITATION

In the equilibrium state, the magnetization lies along the longitudinal axis. An MR signal is detected as a voltage in a receiver coil, induced by the precessing transverse magnetization. Before such a signal can be observed it is necessary to manipulate, or excite, the magnetization out of equilibrium state so that a component in the transverse plane is present.

4.1. Nutation of Magnetization

If an additional field, $\mathbf{B_1}$, is applied in a transverse direction, as shown in Fig. 4, the magnetization will precess about the vector sum of the fields $\mathbf{B_0}$ and $\mathbf{B_1}$. Typically the transverse magnetic field, $\mathbf{B_1}$, is small in amplitude compared with the static field $\mathbf{B_0}$. Thus the perturbation of the

Table 1. List of Biologically Relevant Elements that are Candidates for Producing MR Images with their Key Parameters.

Nucleus	Abundance in Human Body (mole/liter)	Magnetic Moment	γ (MHz/T)	Relative Sensitivity
1-hydrogen, ^{1}H	88	2.793	42.58	1
23-sodium, ^{23}Na	80×10^{-3}	2.216	11.27	1×10^{-4}
31-phosphorus, ^{31}P	75×10^{-3}	1.131	17.25	6×10^{-5}
17-oxygen, ^{17}O	16×10^{-3}	-1.893	-5.77	9×10^{-6}
19-fluorine, ^{19}F	4×10^{-6}	2.627	40.08	3×10^{-8}

Notes: Hydrogen, having the largest magnetic moment and greatest abundance is, by far the best element for general clinical utility. Other elements, such ^{23}Na and ^{31}P, have been used for imaging in limited situations, despite their relatively low sensitivity. A negative sign for the magnetic moment and the gyromagnetic ratio, γ, of ^{17}O refers to the fact that the magnetic moment is anti-parallel to the angular momentum.

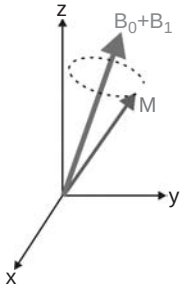

Figure 4. When a static transverse field, $\mathbf{B_1}$, is applied, the magnetization precesses about the vector sum of the field $\mathbf{B_0}$ and $\mathbf{B_1}$. Since $\mathbf{B_1}$ is much smaller than $\mathbf{B_0}$, the effect of a static $\mathbf{B_1}$ is insignificant. (This figure is available in full color at http://www.mrw.interscience.wiley.com/ebe.)

magnetization toward the transverse plane is not relevant if $\mathbf{B_1}$ is static.

The transmitter coils are normally configured so that $\mathbf{B_1}$ can be applied with a component in any direction transverse to $\mathbf{B_0}$. In order to tip the magnetization progressively into the transverse plane, the direction of the $\mathbf{B_1}$ field is rotated such that the $\mathbf{B_1}$ follows the precession of the magnetization vector $\mathbf{M}$. Now, instead of precessing around a static $\mathbf{B_0} + \mathbf{B_1}$, the magnetization continues to be tipped toward the transverse plane, as shown in Fig. 5.

Figure 6 shows a three-dimensional representation of the trajectory defined by the spin for the excitation process during the application of so-called 45°, 90° and a 170° radiofrequency excitation pulses, i.e., RF pulses of intensity and duration such, that they tilt the magnetization vector out of equilibrium orientation by the corresponding angle.

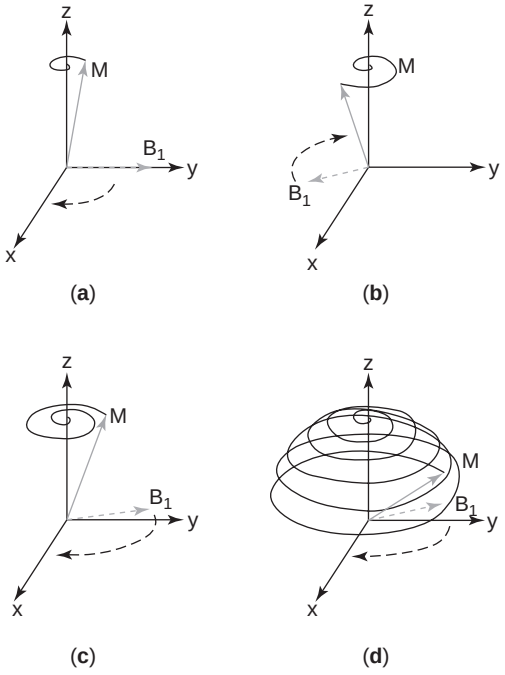

Figure 5. When the direction of the transverse field, $\mathbf{B_1}$, is rotated about $\mathbf{B_0}$ at the same rate as the precession of the magnetization, the transverse field causes the magnetization to tip through a large, controllable angle as shown by the time series (a–d). (This figure is available in full color at http://www.mrw.interscience.wiley.com/ebe.)

4.2. Rotating Magnetic Frame

The process of excitation can be viewed conveniently in a rotating coordinate frame, assuming that the coordinate system *x*-*y*-*z* rotates about the *z*-axis with respect to the still coordinate frame or "laboratory coordinate frame", *x'*-*y'*-*z*. The rotation is at the Larmor rate ω_0 so that a magnetization precessing at a rate of ω_0, for now ignoring relaxation effects, is stationary in the rotating frame. Figure 7a reviews the excitation process in the lab frame (shown in Fig. 5). However, in the rotating frame (Figure 7b) where effectively $\mathbf{B_0} = 0$, $\mathbf{B_1}$ is constant, and the magnetization tips from the longitudinal axis smoothly to the transverse plane with an angular speed proportional to $||\mathbf{B_1}||$.

The resonance frequency of hydrogen at 1.5 T is 63.8 MHz, which is in the radiofrequency band. For this reason, the $\mathbf{B_1}$ field is also referred to as the RF field, and the electrical pulses used to generate it are referred to as RF pulses.

5. RELAXATION

The last two terms of the Bloch equations (Equation 1) describe relaxation of magnetization, the dynamics of how a perturbed magnetization returns to its equilibrium position. If a bar magnet is tilted away from its alignment with a magnetic field it will try to return to its equilibrium state. The net magnetization arising from the protons will do the same, providing two types of relaxation:

- Longitudinal Relaxation – Restoration of longitudinal magnetization to its equilibrium value (T_1 or "spin-lattice" relaxation). It describes an exponential growth (see Fig. 8a).
- Transverse Relaxation – The net magnetization leaving the transverse plane (T_2 or "spin-spin" relaxation) describes an exponential decay (see Fig. 8b).

Longitudinal relaxation results from "spin-lattice" interactions, and results in an exponential recovery of the equilibrium magnetization.

Viewed from a rotating reference frame, longitudinal relaxation of magnetization over a time interval, *t*, gives

$$\mathbf{M_z}(t) = \mathbf{M_0} + (\mathrm{M_z}(0) - \mathbf{M_0})\mathrm{e}^{-\frac{1}{T_1}}, \tag{3}$$

where $\mathbf{M_z}(0)$ and $\mathbf{M_z}(t)$ are the longitudinal components of the magnetization at the start and end of the interval, $\mathbf{M_0}$ is the equilibrium magnetization, and T_1 is the longitudinal relaxation time constant. The longitudinal magnetization component as a function of time is shown in Figure 8a.

Transverse relaxation comes from "spin-spin" interactions, and results in an exponential decay of the transverse magnetization toward zero (Fig. 8b).

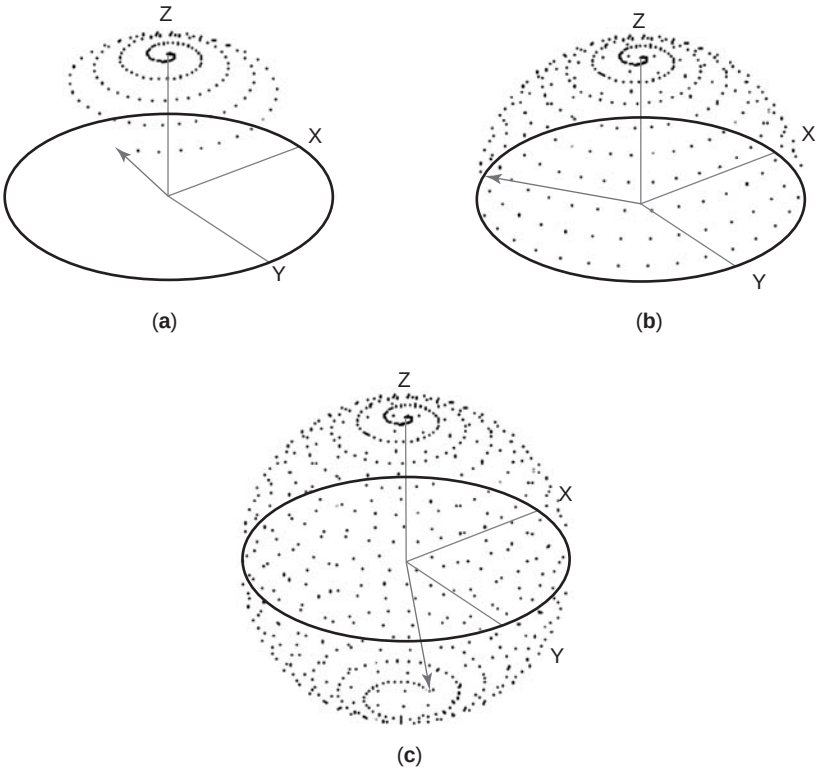

Figure 6. Computer simulated trajectory of the resulting magnetization for the excitation step during the application of a 45° (a), 90° (b) and 170° (c) radiofrequency excitation pulses. (This figure is available in full color at http://www.mrw.interscience.wiley.com/ebe.)

Transverse relaxation over a time interval t gives the transverse magnetization as

$$\mathbf{M_{xy}}(t) = \mathbf{M_{xy}}(0)e^{-\frac{1}{T_2}}, \tag{4}$$

where $\mathbf{M_{xy}}(0)$ and $\mathbf{M_{xy}}(t)$ are the transverse magnetization components of the magnetization at the start and end of the interval, and T_2 is the transverse relaxation time constant. The transverse magnetization due to T_2-relaxation is shown in Fig. 8b.

Longitudinal and transverse relaxation (or T_1-relaxation and T_2-relaxation) are much slower effects than precession. For biological tissues, T_1 and T_2 vary from hundreds of microseconds to several seconds (see Table 2). The difference in relaxation times between different tissue types is frequently exploited as a mechanism of generating contrast between different tissues in imaging. For example, bound water tends to have shorter T_1 and T_2 times than free water (i.e. longitudinal magnetization in bound water will recover faster than in free water, and transverse magnetization decay is faster as well). Pulse sequence parameters, i.e. timing and amplitude parameters for RF and other pulses in an MRI experiment, can be manipulated in a variety of ways to elicit for example predominantly T_1-weighted or T_2-weighted image contrast (see Fig. 9).

The effects of precession and relaxation together are shown in Fig. 10. The transverse component of magnetization disappears with exponential decay time T_2 (Fig. 10a), also called the "spin-spin" relaxation time. The longitudinal equilibrium magnetization recovers decay time T_1

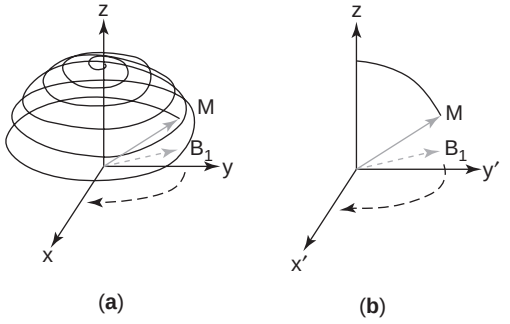

Figure 7. A rotating coordinate frame can be used to show the process of excitation. The rotating frame rotates about the longitudinal axis at the Larmor frequency, ω. When the rotating field **B1** is applied, the magnetization tips in a spiral pattern along a spherical surface in the lab frame (a), but simply moves directly along an arc toward the transverse plane in the rotating frame (b). (This figure is available in full color at http://www.mrw.interscience.wiley.com/ebe.)

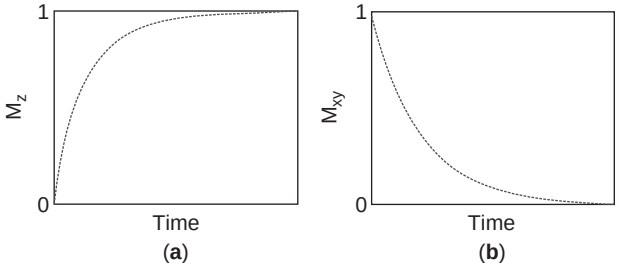

Figure 8. (a) The longitudinal component of magnetization grows exponentially toward its equilibrium value with a time constant T_1. (b) The transverse component of magnetization decays exponentially toward zero with a time constant T_2. (This figure is available in full color at http://www.mrw.interscience.wiley.com/ebe.)

Table 2. Relaxation Times, T_1 and T_2, for Different Body Tissues Under a 1.5 T Magnetic Field Strength, in Milliseconds

Tissue	T_1	T_2
Cerebrospinal Fluid (CSF)	2400	160
Blood	1200	100
White Matter (WM)	780	90
Grey Matter (GM)	920	100
Fat	260	80
Bone marrow	400	60
Muscle	870	45
Liver	500	45
Pancreas	600	70

(Fig. 10b), also called "spin-lattice" relaxation time. It is interesting to point out that T_1 is always greater or equal to T_2 because $||\boldsymbol{M}||$ cannot grow beyond $||\boldsymbol{M}_0||$ during relaxation, and, as defined in the Bloch equations (Equation 1), transverse T_2 relaxation also includes transverse magnetization decay due to T_1 relaxation.

Decay of transverse magnetization may be explained to stem from the fact that different individual spins may precess at slightly different angular speeds, resulting from differences in net magnetic field due to presence of other spins. Over time this destroys the initial phase coherence of the spins following excitation, and this de-phasing results in decay of the net aggregate magnetization in the transverse plane (see Fig. 11b–d)eventually leading to complete cancellation of the signal, as can be observed in Fig. 11e.

Similar to this "true" T_2 relaxation due to the physical properties of the system, inhomogeneity of the main field $\mathbf{B_0}$, due to imperfect instrumentation, causes spins at different locations to precess at slightly different Larmor frequencies. The resulting faster decay of transverse magnetization can be described by another, shorter, relaxation time parameter known as T_2^*, which incorporates combined effects of the natural dephasing and $\mathbf{B}_0$ inhomogeneity.

5.1. Spin Echoes

Dephasing of magnetization in a collection of spins caused by static field inhomogeneities, as described above characterized by the shorter T_2^* relaxation time, does not provide information about the characteristics of the spins involved in the process, and is thus in many instances less interesting than observation of true T_2 decay. If spins are, in a macroscopic sense, at a fixed location, the T_2^* decay of transverse magnetization will proceed at stationary rate in each location. After partial or complete T_2^* relaxation, an appropriately applied pulse applied at a time $t = TE/2$ (TE: echo time) after excitation can invert the transverse component of the magnetization, intrinsically also inverting the accumulated T_2^* phase differences. The inversion thus puts the faster spins behind the slower spins. Upon further evolution of the spin phase distribution the faster spins will catch up with the slower ones and all will be back in phase again, forming a so-called spin echo (Fig. 12e) time at TE after excitation. True T_2 dephasing, which originates from interactions between individual spins, does not recover following inversion by the 180° pulse, and the magnetization that can be observed at the echo time $t = TE$ will follow the decay as described by Equation 4.

6. MAGNETIC RESONANCE IMAGING: SPATIAL ENCODING

The Larmor frequency is proportional to the magnetic field strength. If we subject a spatially distributed sample to a field with a spatially variable field strength, the spectral distribution of the received signal will reflect the spatial characteristics of the sample. This idea, with use of linearly varying fields, is used to great advantage in the medical imaging technique known as magnetic resonance imaging or MRI.

A "gradient field" is generally understood not to change the direction of $\mathbf{B_0}$, but it spatially modulates the $\mathbf{B_0}$ field strength. If a constant (often denoted as "linear") field gradient $\mathbf{G_x}$ is applied in a direction $\mathbf{x}$, the resonance frequency of a collection of identical spins will vary in linear fashion with their position along the x-axis: $\omega(x) = \gamma(\mathbf{B_0} + \mathbf{G_x} \cdot x)$. As illustrated in Fig. 13, it will be possible to recover the spatial distribution of spin signals along this gradient direction $\mathbf{x}$.

6.1. Image Reconstruction from Projections

Define a spin density function $\rho(\mathbf{x})$ in 3-space. If all signal observations may be assumed to be performed within a short time approximately at time t after excitation,

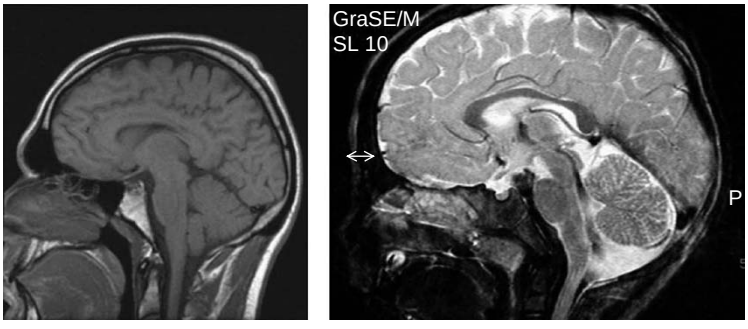

(a) (b)

Figure 9. Head sagital acquisition. (a) T1-weighted image (the cerebrospinal fluid is black), (b) T2-weighted image (the cerebrospinal fluid is white).

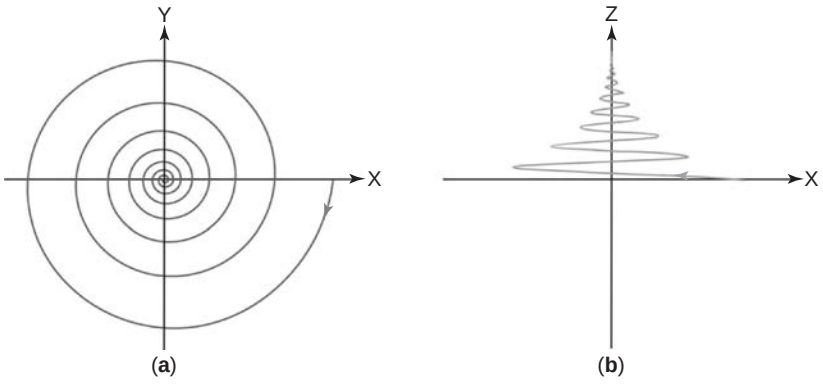

Figure 10. (a) Top and (b) transverse view of idealized "free-precession" of magnetization. As the magnetization relaxes, it precesses about the direction of the applied magnetic field (z-axis, in this case), while returning to its initial equilibrium position. (This figure is available in full color at http://www.mrw.interscience.wiley.com/ebe.)

relaxation properties may be assumed constant during signal detection. We will introduce an "observable image function" f($\mathbf{x}$), which represents the spin density $\rho(\mathbf{x})$, modulated by the relaxation state at this time t. Relaxation contrast will be discussed further in Section *Contrast in NMR Imaging*.

The magnetization vector *s(t)* following excitation will be an integral combination of the spatially distributed resonance frequencies along the gradient direction:

$$s(t) = \int_{-\infty}^{\infty} f(x) e^{-2\pi j \gamma (B_0 + G_x x)t} d_x. \tag{5}$$

After demodulation of the common Larmor frequency (Equation 2) a Fourier transform of the signal will yield the image function *f(x)*, resolved along the gradient direction. Since the field is constant in directions orthogonal to x, this one-dimensional image is a projection of the more-dimensional *f(x)* onto the gradient direction axis.

If a scalable gradient field can be applied independently and concurrently in any of all three main axis directions in 3-space, a gradient in any arbitrary direction may be created as a vector sum of these three gradients.

A complete multi-dimensional image *f(x)* may be reconstructed from a set of such projections, acquired at equidistant angular gradient direction steps, through projection reconstruction methods, based on the Radon Transform [See RADON TRANSFORM] in two or three dimensions.

6.1.1. First Dimension (z): Slice Selection. The $\mathbf{B_1}$ field must be tuned to the resonant frequency of the magnetization. By using gradient fields, a spatial variation can be applied to this resonance frequency. Then, applying a narrow bandwidth RF field, it will excite only a thin "slice" of spins in the object, as shown in Fig. 14. The width of the slice can be decreased either by increasing the amplitude of the gradient field or by decreasing the bandwidth of the RF pulse. The bandwidth of the pulse can be made small

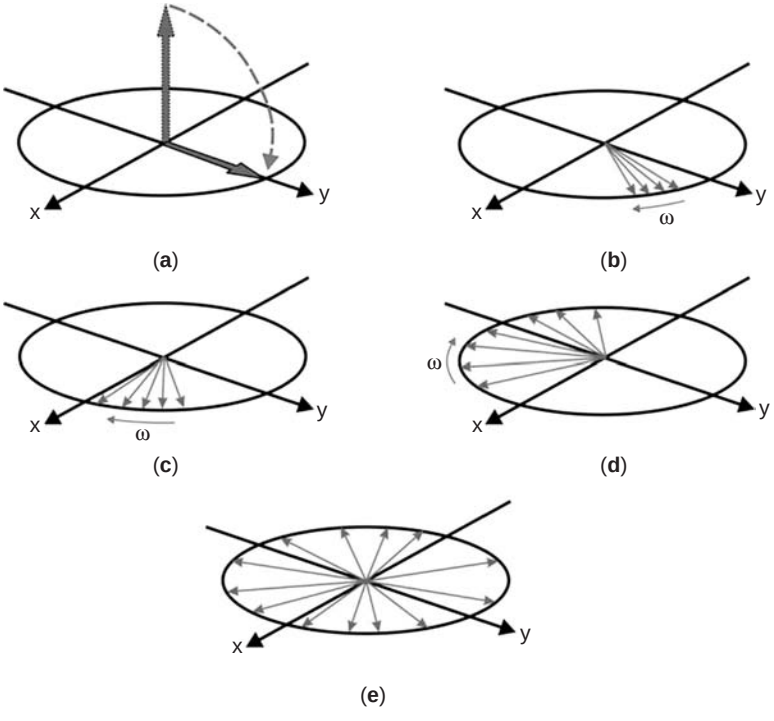

Figure 11. Decay of transverse magnetization. As time goes on and after a 90° excitation pulse (a) the different components of the magnetization precess at slightly different rates (b-d) leading to a complete cancellation of the signal in the transverse plane (e). (This figure is available in full color at http://www.mrw.interscience.wiley.com/ebe.)

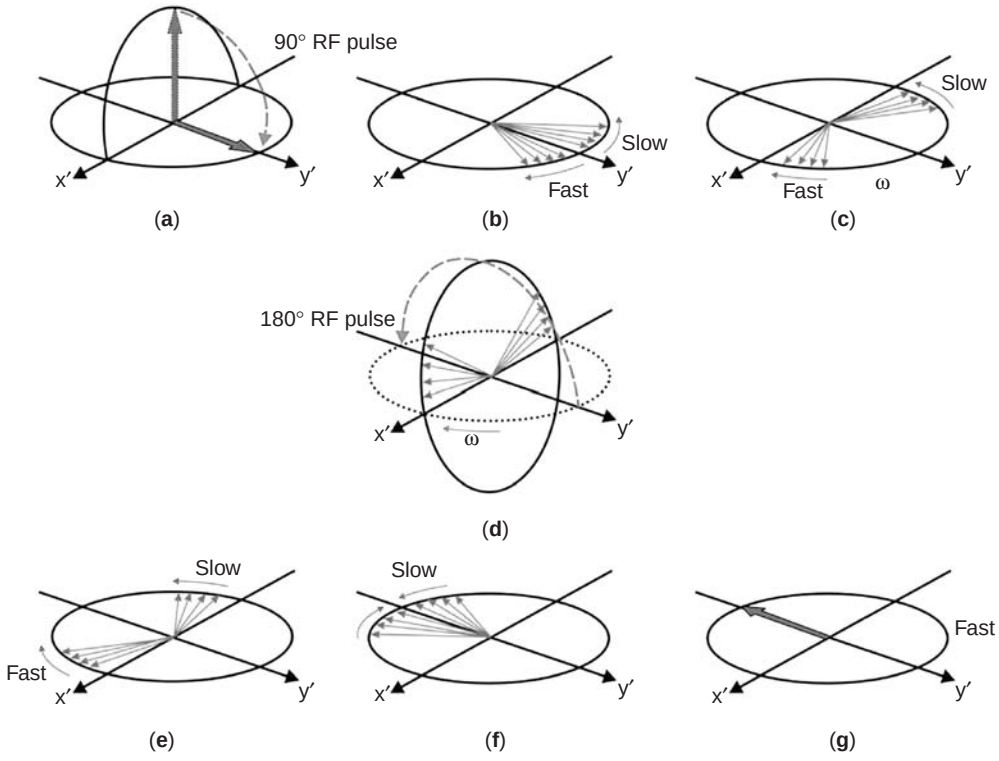

Figure 12. Echo formation in a rotating coordinate frame. After applying a 90° excitation pulse (a), and before all the transverse magnetization has disappeared, a 180° excitation pulse is applied (d), rephasing all magnetization vectors and arising into another vector sum, called the spin echo (g). (This figure is available in full color at http://www.mrw.interscience.wiley.com/ebe.)

at the cost of duration of the pulse. The gradient amplitude is limited by gradient hardware. Typical slice widths in imaging range from 1 to 10 mm.

Similarly, the fact that lipid tissue and water tissue have different resonant frequencies can be exploited. If the RF pulse is made narrow compared to the resonant frequency difference between water and fat, then it is possible to excite water or fat without exciting the other. This is very useful in medical imaging to increase sensitivity to pathological abnormalities by increasing the dynamic range of the MR images.

6.1.2. Second dimension (x): Frequency Encoding. Once the desired slice has been selected, a second gradient, the x-gradient, will be applied during the recording of the echo, implying an instantaneous change of precession frequency, as depicted in Fig. 15.

The NMR signal from each x-position contains a specific center frequency. The over-all NMR signal is the sum of signals along x. A Fourier transform will recover signal contribution at each frequency, i.e. x-location, and the resulting spectrum will determine a projection of the desired imaged object, as shown in Fig. 16.

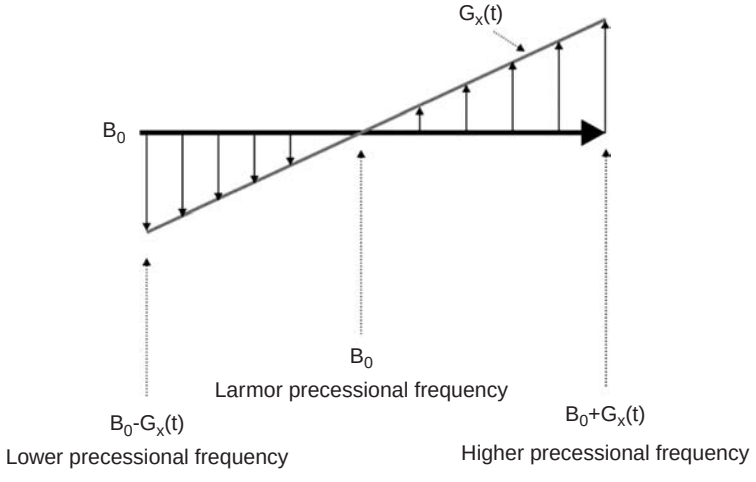

Figure 13. Larmor frequency varies linearly in space. The gradient $\mathbf{G_x(t)}$ creates a spatial variation of the main static field $\mathbf{B_0}$ along direction x over the time t. (This figure is available in full color at http://www.mrw.interscience.wiley.com/ebe.)

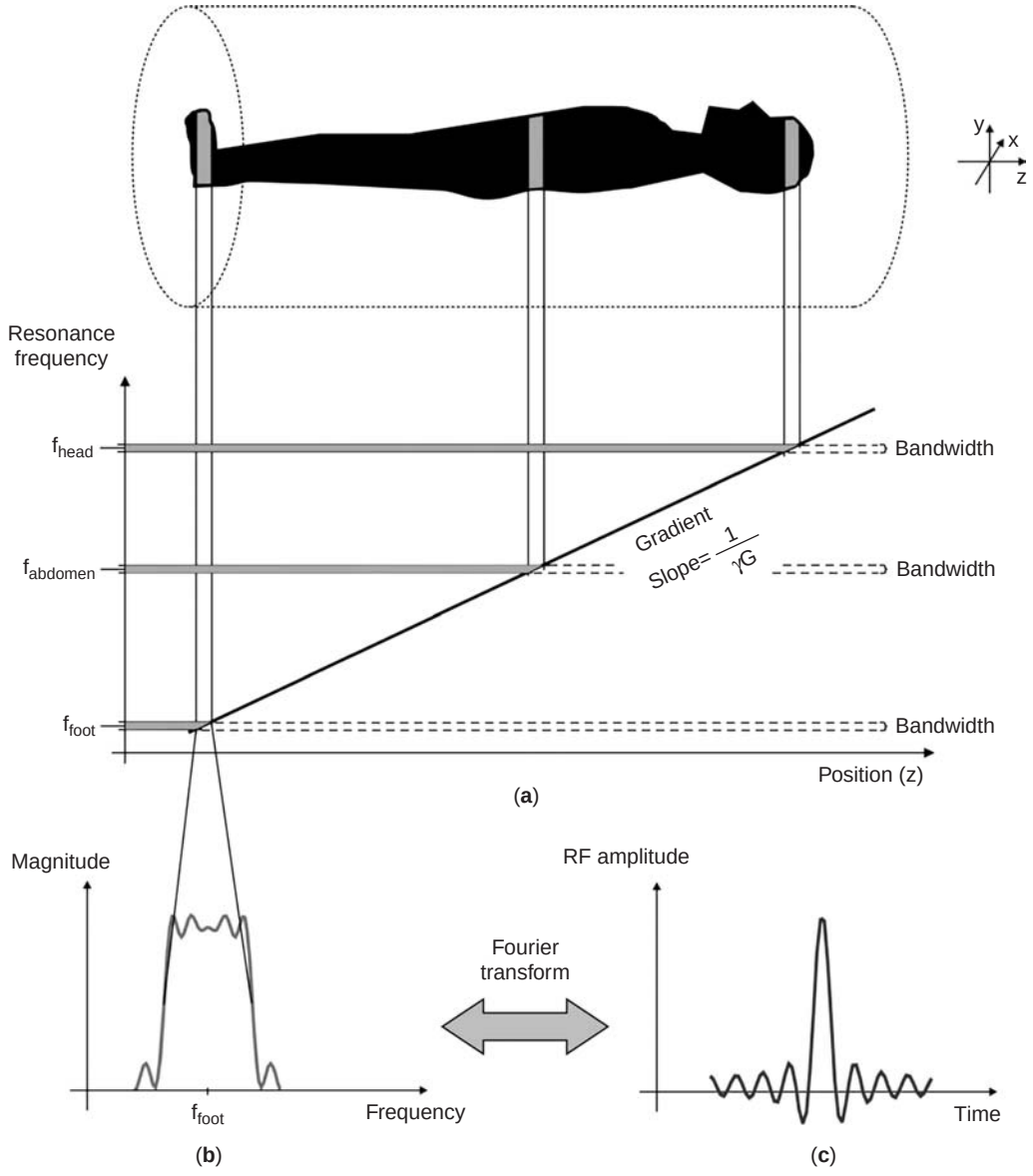

Figure 14. Using a magnetic field gradient (a), a thin slice of tissue can be excited (b) by applying a narrow-band RF pulse that has the frequency profile shown in (c). To a first order approximation, the RF pulse (c) is the Fourier transform of the frequency profile. The width of the slice can be modified by changing the gradient amplitude or the bandwidth of the RF pulse. The slice position can be varied by shifting the modulation frequency of the RF pulse. (This figure is available in full color at http://www.mrw.interscience.wiley.com/ebe.)

6.1.3. Third Dimension (y): Phase Encoding. The frequency encoding gradient (*x*-direction) will always produce iso-lines of resonance frequencies so, how can the *y*-localization be achieved?

There are two very different solutions to achieve the third dimension localization:

1. By reconstructing from several projections using rotating gradients.
2. By using a third encoding gradient: the phase encoding gradient.

Let's study both solutions in order to select the best option.

6.1.3.1. Reconstruction from Projections: Rotating Gradients. When a rotating field gradient is used, linear positioning information is collected along a number of different directions, as shown in Fig. 17. That information can be combined to produce a two-dimensional map of the proton densities. The proton NMR signals are quite sensitive to differences in proton content that are characteristic of different kinds of tissue. Even though the spatial resolution of MRI is not as great as a conventional x-ray film, its contrast resolution is much higher for tissue. Rapid scanning and computer reconstruction give well-resolved images of organs.

The rotating gradients have important disadvantages as the difficulty in acquiring several projections that

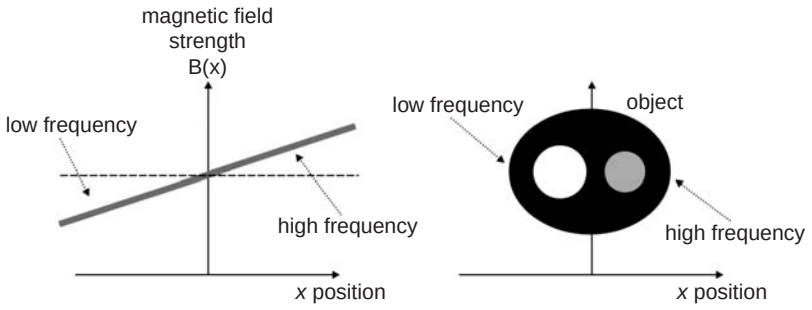

Figure 15. Larmor frequency varies linearly along x-axis: $\omega(x) = \gamma(\mathbf{B_0} + \mathbf{G_x} \cdot x)$. (This figure is available in full color at http://www.mrw.interscience.wiley.com/ebe.)

always go through the same point and the multiple artifacts they create in the image due to its inherent rotation, degrading the final image quality.

Considering also other aspects as the possibility to use a 2D Fourier Transform instead of the filtered backprojection reconstruction, a third gradient has been imposed. This third gradient is known as the phase-encoding gradient.

6.1.3.2. Third Encoding Gradient: the Phase Encoding Gradient. After applying a gradient in y-direction, the nuclei collect different amounts of phase shift φ_y according to y-location: $\varphi(y) = \varphi_y = TP \times \omega(y) = TP \times \gamma G_y \cdot y$ where TP corresponds to the sampling interval in the y-direction.

Application of repeated pulse sequences with y-gradients of increasing steepness (while the frequency-encoding and the slice-encoding gradient stays same) creates a dependence of $\mathbf{B_y}$ (and therefore φ_y) on y-position and the pulse sequence repetition number.

Each position causes a signal component with a unique precession frequency and phase (see Fig. 18), $sin(\Delta\omega_x t + \varphi_y)$. So, for a fixed x-position, the sequence of phase encoding gradients i, from 1 to N, leads to a sine wave like $sin(\Delta\omega_x t + i \times \varphi_y) = sin(c + i \times \omega_y \times TP)$ where $c = \Delta\omega_x t =$ constant, and TP corresponds to the sampling interval in the y-direction.

The 2D array of NMR signals obtained from the frequency and phase readings is referred to as the k-space map.

7. RESOLUTION AND FIELD OF VIEW IN NMR IMAGING

In order to study the basic image parameters like resolution and field-of-view (FOV), the complementary k-space must be considered as summarized in Fig. 19.

The *FOV* determines the dimension of the image, and is typically measured in millimeters. It is directly related to the spacing or density of sampling of data points in k-domain, Δk.

2D image resolution (Δx or pixel size in x-direction, Δy or pixel size in y-direction) is defined as the minimum distance that two point sources can be resolved. It is typically measured in millimeters, and it is related to the highest observed spatial frequency component in k-space, k_x^{max}, both in x-direction and k_y^{max} in y-direction, measured in cycles/cm. *FOV*, k^{max} and Δk are defined in Fig. 20.

The relationship between these parameters is simple. In each case, the extent in one domain multiplied by the resolution in the other domain is unity. Hence

$$FOV_x \times \Delta k_x = 1$$

and

$$2k_x^{max} \times \Delta x = 1.$$

since the extent in k-space goes from $-k_x^{max}$ to $+k_x^{max}$. In addition, if N is the number of samples in either domain, then

$$FOV_x = N_x \times \Delta x$$

and

$$2k_x^{max} = N_x \times \Delta k_x.$$

These equations make intuitive sense if you consider the effect of phase encoding steps for the case of the y-dimension. Each step adds one cycle of phase shift across the FOV. If one phase one encode is zero, then the next at $+\Delta k_y$ produces one cycle over the FOV, so $\Delta k_y = \frac{1}{FOV_y}$ and $FOV_y \times \Delta k_y = 1$.

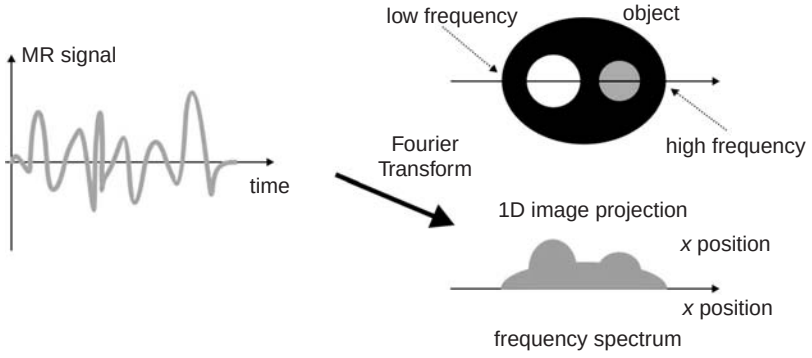

Figure 16. Applying a frequency encoding gradient in x-direction the MR signal obtained is a "modulated" signal that contains information of the 1D image projection of the object through the x-direction. Through a Fourier Transform the useful information can be extracted. The frequency spectrum represents that 1D image projection of the object analyzed through that direction. (This figure is available in full color at http://www.mrw.interscience.wiley.com/ebe.)

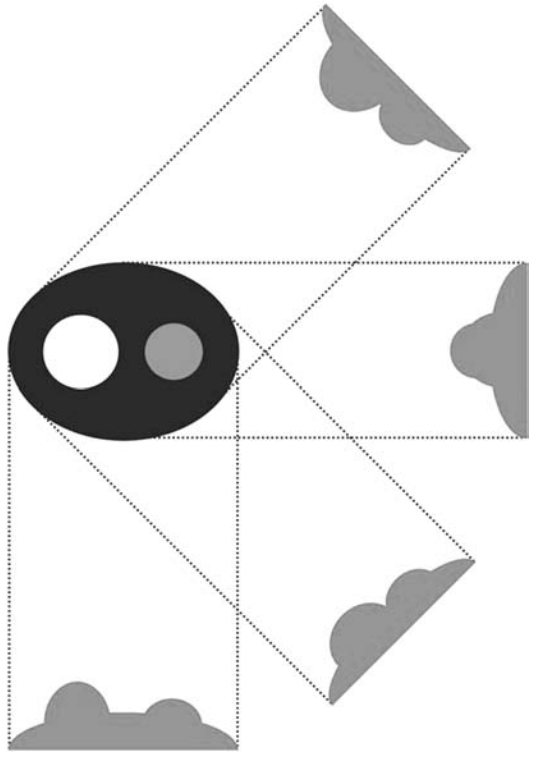

Figure 17. Through rotating gradients, several 1D projections can be obtained. Using filtered backprojection reconstruction, the final image can be reconstructed. (This figure is available in full color at http://www.mrw.interscience.wiley.com/ebe.)

8. MRI HARDWARE

In a conventional MRI system there are some important hardware components that interact directly with the material being scanned:

- A strong static magnetic field in the "longitudinal" direction is produced typically by either a permanent magnet or a superconducting electromagnet.
- A second coil arrangement produces a field, transverse to the static field, that can change with time.
- Receiver coils are also arranged to sense the field in the transverse direction.
- Gradient coils produce a spatial variation of the longitudinal magnetic field with respect to position along three orthogonal axes (see Fig. 21).

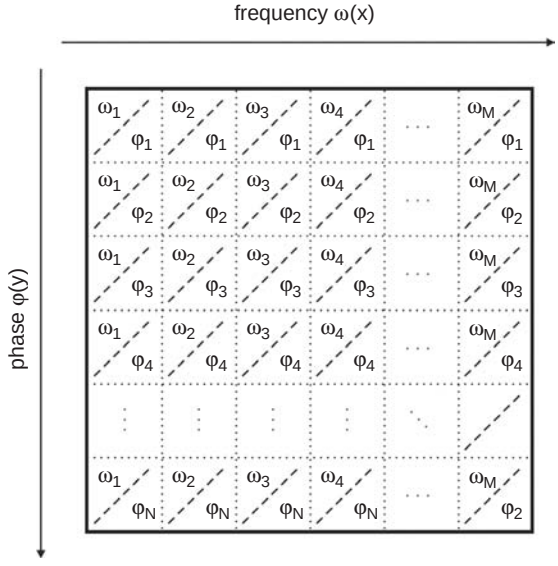

Figure 18. Each position causes a signal component with a unique precession frequency and phase. With the application of the frequency-encoding and the phase-encoding gradients it will be possible to cover the entire matrix.

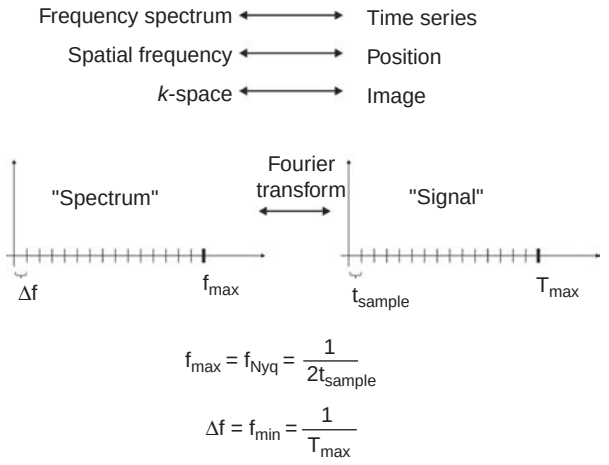

Figure 19. Existing relationships between *k*-space and image space.

8.1. Static Magnetic Field: B_0

The static longitudinal magnetic field $\mathbf{B_0}$ is usually produced either by a superconducting electromagnet or by a permanent magnet. For imaging, it is important that the static field strength be uniform. A stronger static field results in greater polarization of nuclear spins and thus a stronger magnetic resonance signal. The more uniform the static field is, the less the resonant frequency varies with position. Field inhomogeneities cause many difficulties in imaging, from image distortion to blurring and replication artifacts. Typically, the static magnetic field strength of imaging systems ranges from about 0.15 T to as much as 9.7 T, and the homogeneity is better than 1 ppm across the imaging region.

8.2. Transverse Radio Frequency Field: B_1

A transverse, or $\mathbf{B_1}$, field is produced in a direction perpendicular to the static $\mathbf{B_0}$ field. The $\mathbf{B_1}$ field is produced by coils tuned to the resonant frequency of the magnetization. As mentioned above, since this frequency is in the RF band, the coils are often referred to as RF coils. The field from the RF coils is used to excite the magnetization, that is, to "tip" it from its equilibrium position along $\mathbf{B_0}$ to a position where it has a transverse component.

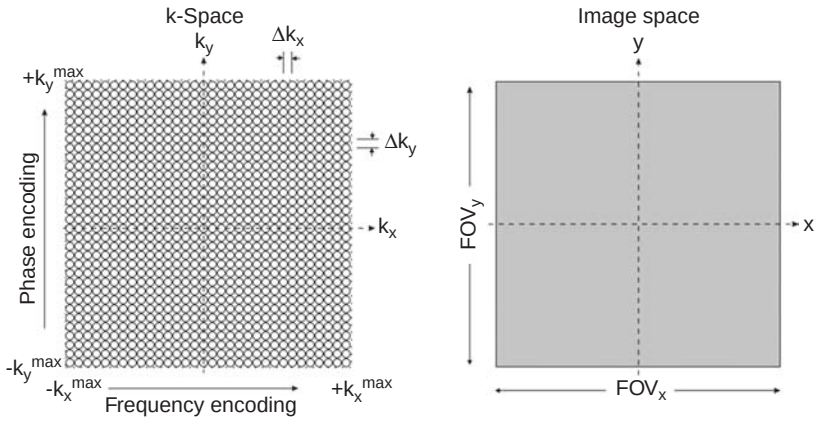

Figure 20. Definition of k^{max} and Δk in k-space in both directions, and *FOV* in image space.

8.2.1. Signal Reception. Precessing transverse magnetization causes a changing flux in a coil oriented facing a transverse direction. Through Faraday's law of induction, this changing flux induces a voltage in the coil (see Fig. 22). The received signal is in the same frequency band as the excitation pulses and often the same coil or coils used to generate the $\mathbf{B_1}$ field can be used to receive the signal.

The received signal can be expressed as a complex valued signal, with the real and imaginary parts representing orthogonal directions in the transverse plane. In this representation, a magnetization resonating at a frequency ω_0 produces a received signal $s_r(t) = e^{-j\omega_0 t}$, where t is time.

This received signal (voltage induced in the receiver coil) is known as a Free Induction Decay or FID:

- "Free": this signal is acquired without the driving $\mathbf{B_1}$ field at the time of observation,
- "Induction": this signal is induced in the coil,
- "Decay": the signal decays exponentially over time at rate T_2^* due to spin-spin relaxation (dephasing) and local field inhomogeneities.

8.3. Spatial-Encoding Gradients

Gradient coils are what enable an MR system to resolve spatial position, and thus form images. Three separate gradient coils provide a linear variation in the longitudinal field strength (Fig. 23) as a function of position along three orthogonal directions. The strength of each gradient can be varied, so that a three-dimensional "gradient-vector" can point in an arbitrary direction and be of arbitrary strength.

The determination of spatially localized MR information depends upon the sequential application of the three pulsed magnetic gradient fields ($\mathbf{G_x}$, $\mathbf{G_y}$ and $\mathbf{G_z}$). These gradients are needed to obtain:

- *Slice selection*: any plane can be selectively excited by applying a magnetic field gradient $\mathbf{G_z}$ during RF excitation.
- *Phase encoding*: following selective excitation, the rotating spins can have their precessional phases manipulated by the $\mathbf{G_y}$ gradient such that they become a function of y.
- *Frequency encoding*: following this phase encoding step all spins are rotating at the same Larmor frequency but at different phases in their precessional orbits. By applying a field gradient in the x-direction ($\mathbf{G_x}$) the Larmor frequency can be manipulated such that it becomes a function of x. Immediately following the application of this field gradient the FID is recorded.

The result of the gradient fields is to produce a variation of the longitudinal component of the magnetic field ($\mathbf{B_z}$) with position:

$$\mathbf{B_z} = |\mathbf{B_0}| + \mathbf{G} \cdot \mathbf{r}, \tag{6}$$

where $\mathbf{G}$ is the gradient vector and $\mathbf{r}$ is a position vector, with respect to a central origin where the gradients have no effect on the field. The variation of longitudinal field strength results in a corresponding linear variation of resonant frequency with position. This resonant frequency difference is what is used to resolve position in images.

9. CONTRAST IN NMR IMAGING

The intensity or brightness of a position in an image is a reflection of the amplitude of the MR signal arising from that position, which in turn is proportional to the concentration of mobile protons at that position. The ability of MR to not only map the tissue proton density but also to sense other alterations in its chemical structure is the main factor that distinguish MR from other imaging techniques. This ability resides in the fact that different tissues have different T_1 and T_2 values. Especially for pathological tissue, these values are substantially modified, permitting its use as a source of contrast. The change can be as large enough as to produce a great contrast difference between pathologic and normal tissues. This allows the design of highly specific imaging sequences and weightings, directed to the detection of particular abnormalities.

There are different ways of modifying contrast depending on the nature of the property on which it is based either the intrinsic properties of the biological tissue (relaxation times T_1 and T_2, proton density, chemical shift, flow) or the extrinsic properties of the sequence (repetition time between pulse sequences, echo time, flip angle).

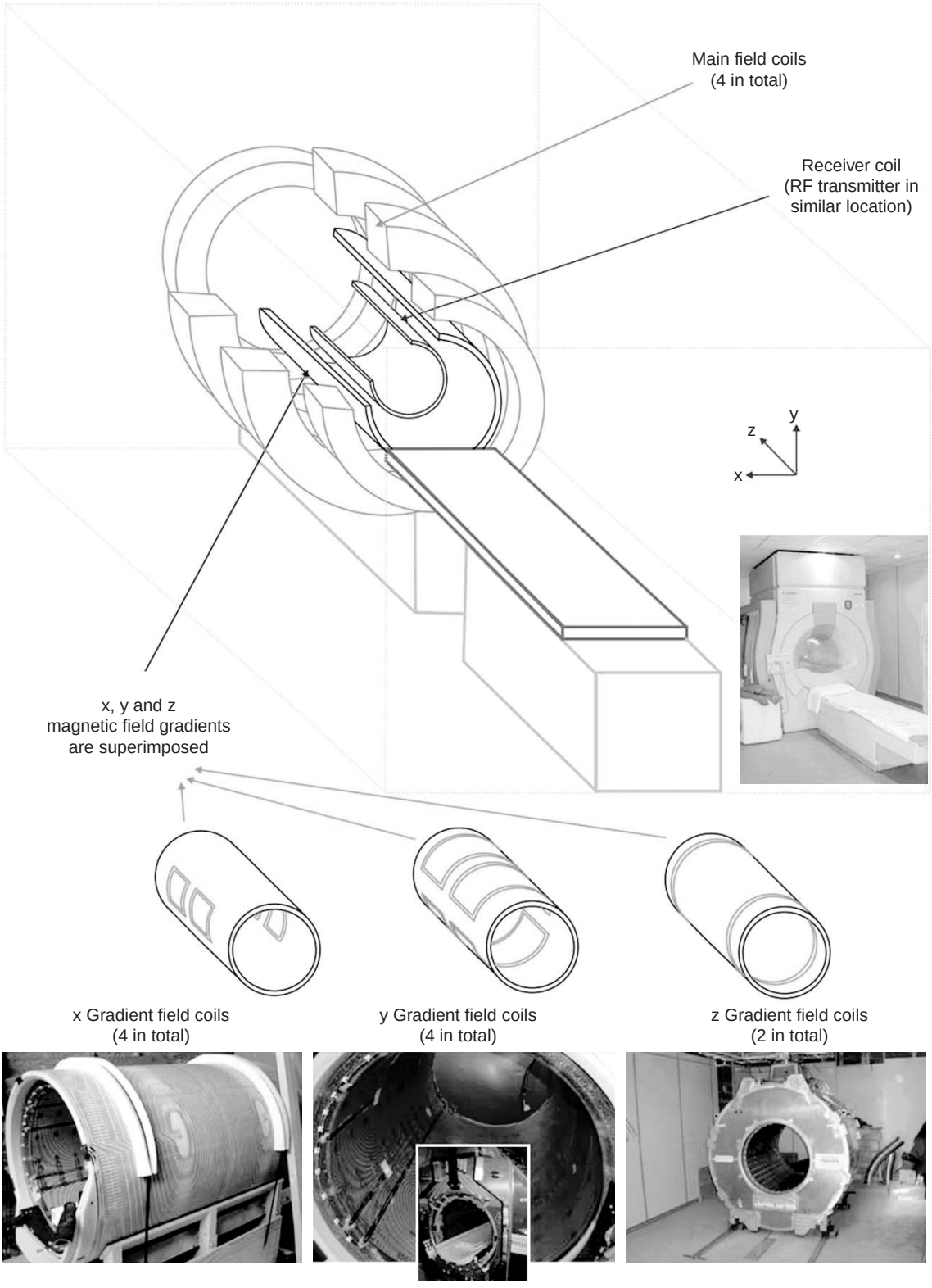

Figure 21. Arrangement of magnets in an MRI machine. (This figure is available in full color at http://www.mrw.interscience.wiley.com/ebe.)

Figure 24 shows the T_1 and T_2 relaxation times curves for two different tissues, and Table 3 gives some indications for the influence of TR and for TE in order to obtain T_1, T_2 or spin density weighted images.

9.1. T2 Weighted Imaging

In order to obtain contrast according to different T_2 values, we must manipulate the TR (time between repetitions of a

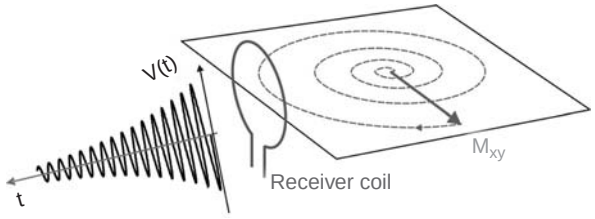

Figure 22. Detecting the magnetization. Imagine that a 90° pulse is applied to the collection of spins. The net magnetization will now lie in the transverse plane and begin to precess about the $\mathbf{B_0}$ axis at a rate equal to the Larmor frequency. This macroscopic magnetization is changing direction (rotating) over time, thus it can induce an alternating current in a coil of wire. That current can then be used as a measure of the magnetization in the transverse plane. (This figure is available in full color at http://www.mrw.interscience.wiley.com/ebe.)

pulse sequence) and TE (time from the 90° pulse to the generation of the spin-echo). This is accomplished by setting $TR \gg T_1$ and prolonging TE to the range of tissue values. The long TR will permit complete recovery of longitudinal magnetization regardless of variations in tissue T_1 values. Since the signal is not detected until the time TE after the 90° pulse, the transverse magnetization will have decayed more in a tissue with a short T_2 time as compared to a tissue with a longer T_2 time. Tissues with longer T_2 times will contribute more signal, and therefore appear hyperintense in the MR image relative to tissues with shorter T_2 times.

9.2. T1 Weighted Imaging

T_1-weighted imaging is accomplished by shortening the TR to the range of tissue T_1 values, and making $TE \ll T_2$. The short TE does not allow time for significant decay of the transverse magnetization regardless of tissue T_2 values. However, since TR is short, the amount of longitudinal magnetization available for the next spin-echo excitation/detection sequence depends on how fast it was able to recover from the previous excitation pulse. Therefore, those tissues with short T_1 times will have more longitudinal magnetization available for conversion into transverse magnetization before each excitation pulse. Consequently, tissues with shorter T_1 values contribute more signal and appear hyperintense relative to tissues with longer T_1 values.

10. PULSE SEQUENCES IN MRI

MRI provides the best contrast between tissues among the existing medical imaging modalities. One of the reasons of this great contrast achievable in MRI is found in the variety of parameters that can be modified during the acquisition. Some of these parameters are related to what is known as pulse sequences. A pulse sequence can be described as the temporal succession of RF pulses, determining its temporal occurrence, the flip angle of the RF pulse, its duration, the time line of the application and the duration of the magnetic field gradients, and the moment of the acquisition.

There is a huge amount of MR imaging sequences acronyms and different families but almost all the existing MR sequences and techniques can be classified based on some primary descriptive terms. The following terms have been extracted from the agreement between *Vlaardingerbroek and den Boer* and *Haacke, Brown, Thompson and Venkatesan*, and are shown in Table 4, where the magnetization state and echo number and type of the MR scan method is described. A brief description of each one of the descriptive terms of MR scan methods used in that Table is explained below.

1. Magnetization state
   The magnetization state describes the magnetization at the start of the sequence –just before the excitation pulse-.
   a. unprepared/preparedIn Magnetization-Prepared methods each sequence or group of sequences is preceded by one or more RF pulses and gradient lobes to influence the magnetization state at the start of the sequence. Magnetization preparation is used to influence the weighting of the resulting images and make T_1 or T_2 weighting more dominant. Also, other weighting parameters may be influenced (for example diffusion weighting).

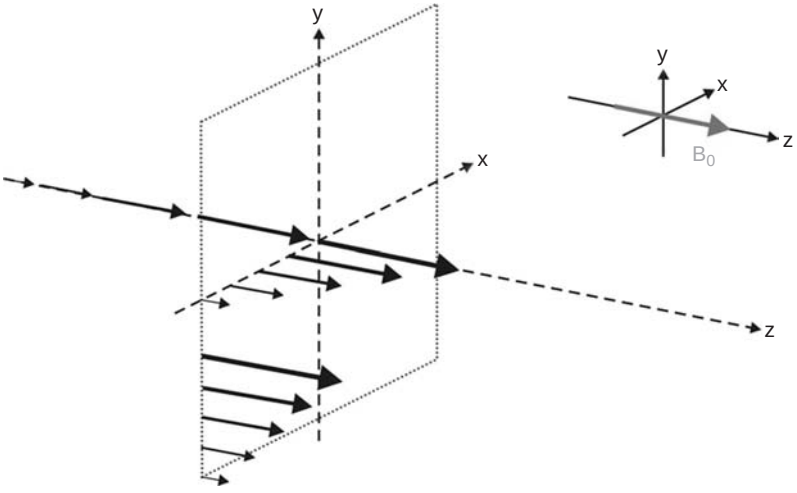

Figure 23. The three gradient components cause the longitudinal field amplitude to vary linearly with position in the direction of the gradient. The arrows in the figure represent the longitudinal field strength at each position along the axis. The amplitude and sign of the gradients can be varied. The gradient vector, $\mathbf{G}$, is generated by three separate coils, $\mathbf{G_x}$, $\mathbf{G_y}$ and $\mathbf{G_z}$. $\mathbf{G_x}$ and $\mathbf{G_y}$ create a variation of $\mathbf{B_z}$ with position in transverse directions while $\mathbf{G_z}$ creates a variation in $\mathbf{B_z}$ with position in the longitudinal or *z*-direction. (This figure is available in full color at http://www.mrw.interscience.wiley.com/ebe.)

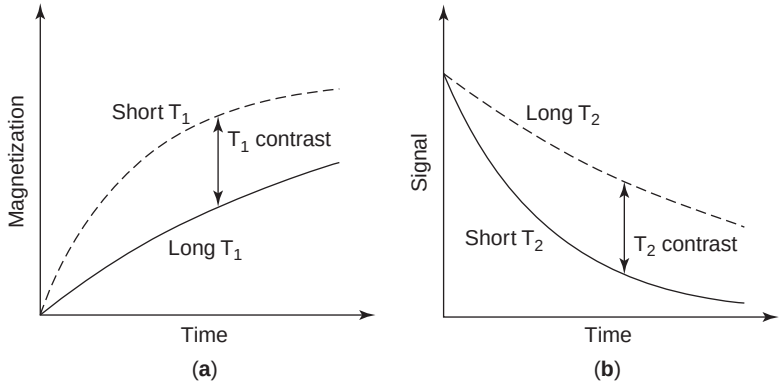

Figure 24. T_1 (a) and T_2 (b) relaxation times for different tissues.

b. ounspoiled/spoiledSpoiling (generated by RF phase cycling of the excitation pulses or by gradients) may be applied to minimize, in the acquired signal, the observed coherence between the contribution of the FID and the transverse magnetization resulting from earlier excitations at the start of each sequence.

c. steady/transientSteady-state methods have an equal magnetization state at the start of each sequence, while transient-state sequences are all sequences in which the magnetization state at the start of each sequence changes, in phase and/or in magnitude.

2. Echo

The excitation pulse with which a sequence starts generates an FID. Normally, this FID is not measured directly, but is transformed into one or more spin echoes and/or gradient echoes, producing either spin echo methods or gradient echo methods – although a mixture of these is also possible-.

a. numberConcerning the number of echoes that can be acquired after each excitation in order to acquire the *k*-space data, there are three different options:

i. it can be sampled one line of the *k*-space after each RF pulse,

ii. or several lines of the *k*-space can be acquired after one RF pulse,

iii. or all the whole *k*-space can be filled after just one RF pulse.The techniques where just one Fourier-encoded is read per TR, as for the first case, will be called single-echo techniques, as in conventional spin-echo or gradient-echo sequences.The techniques that utilize multiple echoes with different Fourier encodings per TR, as for the second and third cases described above, will be called repeated-echo techniques. For these repeated-echo techniques, it will be indicated when the sequence is of the second case (with segmented *k*-space acquisition, widely used, for example, in cardiac imaging) or of the third case (filling the *k*-space after one RF pulse, also known as single-shot techniques, as in most cholangiographic images).

3. type

a. spin echoIn spin-echo imaging the signal immediately after a 90° pulse is not measured but a spin-echo is created using a 180° rephasing pulse.

b. gradient echoAn echo is formed by means of refocusing gradients. Compared to spin-echo sequences, a shorter echo time is possible because no time is needed for the 180° rephasing pulse, although imaging changes caused by dephasing occur more often in this type of scans.

Table 3. Contrast in MRI

	T_2 weighted imaging
Long TR	- Reduces saturation and minimizes influence of different T_1.
Long TE	- Maximizes T_2 contrast. Relatively poor SNR.
	Spin density weighted imaging
Long TR	- Minimizes effects of different degrees of saturation (T_1 contrast). - Maximizes signal
Short TE	- Minimizes T_2 contrast. - Maximizes signal.
	T_1 weighted imaging
Short TR	- Maximizes T_1 contrast due to different degrees of saturation.
Short TE	- Minimizes T_2 influence, maximizes signal.

11. ACCELERATION STRATEGIES IN MRI

MRI is considered a relatively slow medical imaging modality (vs. Computed Tomography, for example) but it is improving very fast. A variety of avenues have been pursued in the quest to reduce the acquisition time and, in addition to important improvements associated with advanced hardware and faster acquisition sequences, the incorporation of various types of prior knowledge to the acquisition and reconstruction steps has been investigated to constrain the reconstruction problem and thus reduce data requirements.

Table 4. Descriptive Terms of MR Scan Methods.

Magnetization State			Echo	
			Number	Type
unprepared prepared	unspoiled spoiled	steady transient	single repeated	spin echo gradient echo

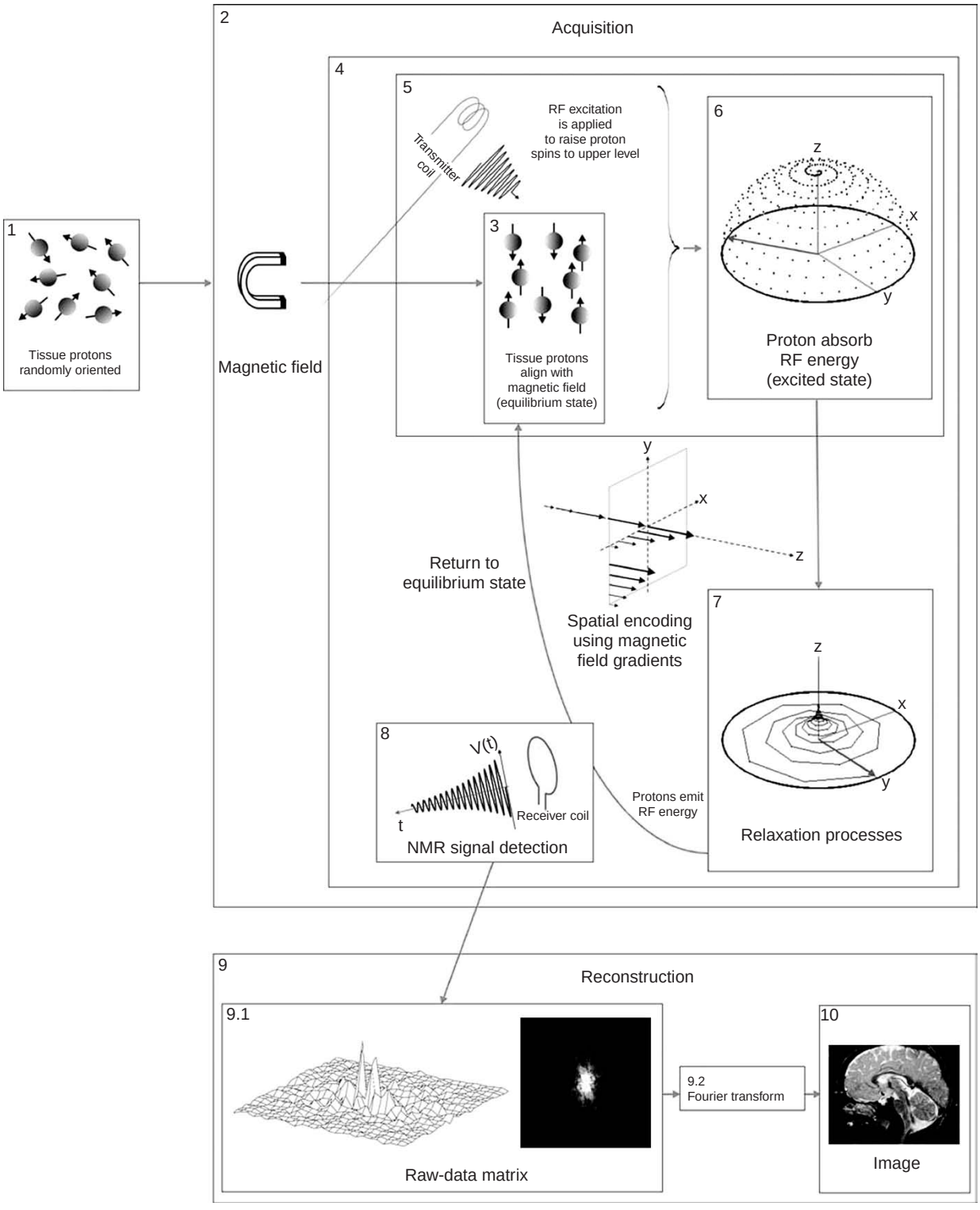

Figure 25. MRI global scheme from spin physics to image reconstruction. (This figure is available in full color at http://www.mrw.interscience.wiley.com/ebe.)

While increasing imaging speed has largely been associated with stronger gradient systems in the past, inherent limitations of ever-faster magnetic field gradients have been reached. These limitations relate to the potential of peripheral nerve stimulation caused by fast switching gradients. Moreover, the total energy deposited in the patient is a concern even at moderate magnetic field strengths, such as 1.5 Tesla. This is of particular relevance if imaging sequences with short repetition times and relatively large flip angles are applied.

With the development of acceleration techniques, alternative ways for speeding up data acquisition have become available. Although there are several different techniques to reduce scan time, most of them can be classified in two big families: view sharing acceleration techniques and parallel imaging techniques.

View-sharing techniques acquire incomplete sets of phase-encodings for different cine images. Then, they share phase-encodings from temporally adjacent acquisitions to complete the *k*-space matrix for each cine phase image. Parallel imaging techniques can be also further divided into two big groups: those that operate in image space and those that operate in *k*-space. By one hand, those working with the image space, with SENSE as its most well-known technique, uses receiver coil array sensitivity maps to compute missing data from an undersampled scan. On the other hand, those from *k*-space, with SMASH as its precursor technique, uses specific receiver coil geometries to create additional *k*-space information without added scans.

12. ADVANTAGES AND DISADVANTAGES OF MRI

MRI has several advantages, some of them unique between the existing medical imaging modalities. Among the most important advantages are:

- It has an excellent soft tissue contrast.
- Pathology and injuries show up well (tumor, hemorrhage, etc).
- Very few artifacts and complete penetration (*vs*. X-ray).
- It is possible to do flow imaging (angiography) and contrast enhancement methods.
- It provides high resolution images (under the mm).
- It is possible to image in any direction.
- Allow specialized applications as spectroscopy or functional MRI.
- It is non-invasive, it uses non ionizing radiation and it has no known hazard.

The main disadvantages are listed below:

- It is relatively slow (*vs*. Computed Tomography, for example) but it is improving very fast.
- Patients must be monitored for implants, pacemakers and electromagnetic devices.
- Possible to have claustrophobia in some MRI designs.

Figure 25 shows a global scheme that tries to explain the whole process in NMR Imaging: from spin physics to image reconstruction.

READING LIST

F. Bloch, W. W. Hansen, and M. E. Packard, Nuclear induction. *Phys. Rev.* 1946; **69**(3-4):127.

M. E. Brummer, D. Moratal-Pérez, C.-Y. Hong, R. I. Pettigrew, J. Millet-Roig, and W. T. Dixon, Noquist: reduced field-of-view imaging by direct fourier inversion. *Magn. Reson. Med.* 2004; **51**:331–342.

M. T. Draney, *In Vivo Quantification of Vessel Wall Motion and Cyclic Strain Using Cine Phase Contrast Magnetic Resonance Imaging.* Thesis report. Stanford University, 2003.

J. L. Duerk, Principles of MR image formation and reconstruction. *Magn. Reson. Imaging Clin. N. Am.* 1999; **7**:629–659.

E. M. Haacke, R. W. Brown, M. R. Thompson, and R. Venkatesan, *Magnetic Resonance Imaging: Physical Principles and Sequence Design*. New York: Wiley-Liss, 1999.

B. A. Hargreaves, *Spin-Manipulation Methods for Efficient Magnetic Resonance Imaging.* Thesis report. Stanford University, 2001.

S. Kozerke and J. Tsao, Reduced data acquisition methods in cardiac imaging. *Top. Magn. Reson. Imaging* 2004; **15**:161–168.

P. C. Lauterbur, Image formation by induced local interactions: examples employing nuclear magnetic resonance. *Nature* 1973: **242**:190–191.

A. Macovski, Noise in MRI. *Magn. Reson. Med.* 1996; **36**:494–497.

K. McLeish and P. Irarrazaval, Scan time reduction with an adaptive field of view. *Magn. Reson. Imaging* 2005; **23**:47–52.

D. Moratal-Pérez, L. Martí-Bonmatí, M. E. Brummer, J. Millet-Roig, and F. Castells, Surcando el espacio-k para mejorar la imagen por resonancia magnética (Exploring k-space for improved MR imaging). *Radiol.* 2004; **46**:133–150. [In Spanish]

D. Moratal-Pérez and V. Denolin, *Normalización y Descripción de Secuencias.* Ediak Med, Barcelona, 2005. [In Spanish]

C. B. Paschal and H. D. Morris, K-Space in the Clinic. *J. Magn. Reson. Imaging* 2004; **19**:145–159.

J. G. Pipe, Basic spin physics. *Magn. Reson. Imaging Clin. N. Am.* 1999; **7**:607–627.

E. M. Purcell, H. C. Torrey, and R. V. Pound, Resonance absorption by nuclear magnetic moments in a solid. *Phys. Rev.* 1946, **69**(1-2):37–38.

P. Reimer, P.M. Parizel, and F.-A. Stichnoth eds., *Clinical MR Imaging A Practical Approach*. Berlin: Springer-Verlag, 1999.

P. A. Rinck ed., *Magnetic Resonance in Medicine. The Basic Textbook of the EMRF.* 3rd ed. Oxford: Blackwell Scientific Publications, 1993.

G. E. Sarty, *Natural K-Plane Coordinate Reconstruction for Magnetic Resonance Imaging Signals.* Thesis report. University of Saskatchewan, Saskatoon, 1995.

M. T. Vlaardingerbroek and J. A. den Boer, *Magnetic Resonance Imaging, Theory and practice.* Berlin: Springer-Verlag, 1996.

NOISE IN INSTRUMENTATION

MIREYA FERNÁNDEZ CHIMENO
MIGUEL ÁNGEL GARCÍA GONZÁLEZ
MANUEL VARGAS DRECHSLER
JUAN JOSÉ RAMOS CASTRO
Universitat Politecnica de Catalunya
Barcelona, Spain

1. INTRODUCTION

The advances in electronics and instrumentation design today allow for extracting the information contained in